



Novel molecular cues for dental defects in hypophosphatasia

Hannah Melms^{a,b}, Marietta Herrmann^{a,c}, Konrad Förstner^{d,e,f}, Richa Bharti^{d,g}, Doris Schneider^a, Birgit Mentrup^{a,h}, Maximilian Rudertⁱ, Ulrich Schlagenhaupt^j, Franz Jakob^{a,1}, Stephanie Graser^{a,*,1}

^a Bernhard-Heine-Center for Locomotion Research, University of Würzburg, Würzburg, Germany

^b Department of Conservative Dentistry, School of Dental Medicine, University Hospital Tübingen, Tübingen, Germany

^c IZKF Research Group Tissue Regeneration in Musculoskeletal Diseases, University Hospital Würzburg, Würzburg, Germany

^d Core Unit SysMed, University of Würzburg, Würzburg, Germany

^e Institute for Information Sciences, University of Applied Sciences, Cologne, Germany

^f ZB MED – Information Centre for Life Science, Cologne, Germany

^g Department for Bioinformatics, Weihenstephan-Triesdorf University of Applied Sciences, TUM Campus Straubing for Biotechnology and Sustainability, Straubing, Germany

^h Department for Regenerative Musculoskeletal Medicine, University of Münster, Germany

ⁱ Department of Orthopaedics, Orthopedic Department König-Ludwig-Haus, University of Würzburg, Würzburg, Germany

^j Department of Periodontology, University Clinics Würzburg, Würzburg, Germany

ARTICLE INFO

Keywords:

Hypophosphatasia
Tissue-nonspecific alkaline phosphatase
Periodontal ligament
Dental pulp
Mesenchymal stem cell

ABSTRACT

Mineralization disorders with a broad range of etiological factors represent a huge challenge in dental diagnosis and therapy. Hypophosphatasia (HPP) belongs to the rare diseases affecting predominantly mineralized tissues, bones and teeth, and occurs due to mutations in the *ALPL* gene, which encodes tissue-nonspecific alkaline phosphatase (TNAP). Here we analyzed stem cells from bone marrow (BMSCs), dental pulp (DPSCs) and periodontal ligament (PDLSCs) in the absence and presence of efficient TNAP inhibitors. The differentiation capacity, expression of surface markers, and gene expression patterns of donor-matched dental cells were compared during this *in vitro* study. Differentiation assays showed efficient osteogenic but low adipogenic differentiation (aD) capacity of PDLSCs and DPSCs. TNAP inhibitor treatment completely abolished the mineralization process during osteogenic differentiation (oD). RNA-seq analysis in PDLSCs, comparing oD with and without TNAP inhibitor levamisole, showed clustered regulation of candidate molecular mechanisms that putatively impaired osteogenesis and mineralization, disequibrated ECM production and turnover, and propagated inflammation. Combined alteration of cementum formation, mineralization, and elastic attachment of teeth to cementum via elastic fibers may explain dental key problems in HPP. Using this *in vitro* model of TNAP deficiency in DPSCs and PDLSCs, we provide novel putative target areas for research on molecular cues for specific dental problems in HPP.

1. Introduction

HPP is a rare, heritable disease caused by mutations in the *ALPL* gene, which encodes the ectoenzyme TNAP. HPP prevalence ranges from 1:300.000 (severe) to 1:6.000–7.000 births (milder manifestations) [1], the clinical phenotype covers a broad range from perinatally lethal cases to late-onset mild symptoms [2]. In the subtype Odonto-HPP, patients only develop a dental phenotype including symptoms like

premature tooth loss without tooth root resorption, defective dentin mineralization, enlarged pulp cavities, and increased prevalence of periodontitis, but interestingly no obvious bone phenotype [3,4]. Substrates of the GPI-anchored enzyme include inorganic pyrophosphate (PP_i), pyridoxal-5-phosphate (PLP), phosphorylated osteopontin (p-OPN) and adenosine tri-/di-/monophosphate (ATP, ADP, AMP) [5,6].

Apart from its well described prevalence in osteoblasts [7], TNAP enzyme can also be detected in dental tissues. In the latter, the enzyme

Abbreviations: aD, adipogenic differentiation; BMSCs, bone marrow mesenchymal stem cells; DPSCs, dental pulp stem cells; ECM, extracellular matrix; GPI, glycosylphosphatidylinositol; GSEA, Gene set enrichment analysis; HPP, hypophosphatasia; Lev, levamisole; oD, osteogenic differentiation; P_i, inorganic phosphate; PDLSCs, periodontal ligament stem cells; PLP, pyridoxal-5-phosphate; PP_i, inorganic pyrophosphate; TNAP, tissue-nonspecific alkaline phosphatase

* Corresponding author.

E-mail address: s-graser.klh@uni-wuerzburg.de (S. Graser).

¹ Both authors contributed equally.

<https://doi.org/10.1016/j.yexcr.2020.112026>

Received 19 December 2019; Received in revised form 15 April 2020; Accepted 17 April 2020

Available online 22 April 2020

0014-4827/ © 2020 The Authors. Published by Elsevier Inc. This is an open access article under the CC BY-NC-ND license

(<http://creativecommons.org/licenses/by-nc-nd/4.0/>).

is produced e.g. in ameloblasts, odontoblasts, and in the periodontal ligament (PDL) [8,9]. Moreover, a role in cementum mineralization has been attributed to TNAP [10]. HPP children frequently show premature loss of deciduous teeth without prior root resorption [11] and impaired mineralization of enamel, dentin, and cementum [12,13].

Mesenchymal stem cells (MSCs) reside in the bone marrow and are discussed and characterized as multipotent stem cells for skeletal regeneration [14]. Their stem cell attributes, regenerative potential, and the nomenclature are presently under debate [15,16]. Similar precursors have been characterized as pulp- or ligament-specific stromal cells (DPSC or PDLSC respectively) [17], which are involved in the formation of the pulp, cementum, periodontal ligament and dentin matrix [18]. Due to their neuroectodermal origin, DPSCs express neuron-related receptors, like those for serotonin and dopamine, which take part in repair processes and TNAP regulation and mineralization [19].

The molecular reasons for the variability of dental symptoms have not yet been completely unraveled. However, Rodrigues et al. have already analyzed the role of P_i/PP_i ratio in developmental processes of the teeth in PDL cells [20] and have detected differential expression of PP_i regulating genes, reduced AP-activity, as well as decreased mineral matrix formation in dental pulp cells of HPP patients [21]. In addition to this, exploiting transcriptomic profiling and models of protein interactive networks from PDL-derived precursor cells, we can show here that the inhibition of TNAP activity in dental precursors allows characterization of new research targets in dental HPP. Changes in signaling pathways related to osteogenesis and mineralization, inflammation, as well as ECM turnover and degradation may help to unravel the underlying molecular pathology of dental HPP and pave the way towards the development of new therapy options.

2. Materials and methods

2.1. Preparation and cultivation of mesenchymal stem cells

Isolation of dental stem cells was performed using an adapted protocol from methods described in the literature [17,22]. Cells were extracted from caries free third molars, after mechanical disruption of the teeth, using 0.4 mg/ml collagenase, 4 mg/ml dispase (Sigma Aldrich) in sterile PBS [23]. Five donor-matched pairs of DPSCs and PDLSCs were collected. Teeth have been extracted in the Department for Conservative Dentistry and Periodontology of the University Clinics Würzburg, Germany (donors' age 13–44, 4 male, 1 female) and were donated under written consent and with permission of the local ethics committee (Permission number: 182/10; from 04/04/2011, extended on the 25/11/2015; Department for Tissue Engineering and Regenerative Medicine of the University of Würzburg, Germany). Isolated cells were cultivated in standard culture medium DMEM Ham's F12 (Life Technologies), 10% FCS (Biocrom), 1% penicillin/streptomycin (Thermo Fisher Scientific) and 50 μ g/ml L-ascorbate-2-phosphate (Sigma Aldrich), which was changed twice a week. For detailed information on the isolation process see appendix.

Bone marrow mesenchymal stem cells (BMSCs) were isolated, as previously described, from femoral heads of healthy donors, who underwent hip arthroplasty in the orthopedic clinic König-Ludwig-Haus in Würzburg [24] and were obtained with permission from the local ethics committee (permission number: 186/18) for control purposes.

2.2. Differentiation of mesenchymal stem cells

Cells were seeded at a density of 5×10^3 cells/cm² in passage 2 (dental stem cells) and 2×10^4 cells/cm² in passage 1 (BMSCs), respectively and grew until confluence. Osteogenic and adipogenic differentiation were performed as previously described [25]. Briefly, osteogenic differentiation medium based on DMEM High Glucose (4.5 g/l) medium to which 10% heat-inactivated FCS (Biocrom GmbH,

Berlin, Germany), 1% penicillin/streptomycin, 50 μ g/ml L-ascorbate-2-phosphate, 10 mM β -glycerophosphate, and 100 nM dexamethasone were added. Adipogenic differentiation medium based on DMEM High Glucose medium and 10% heat-inactivated FCS, 1% penicillin/streptomycin, 1 μ M dexamethasone, 500 μ M 3-isobutyl-1-methylxanthine, 1 μ g/ml insulin, and 100 μ M indomethacin were added. For control purposes, DMEM High Glucose medium, including 10% FCS and 1% penicillin/streptomycin, was used. TNAP inhibitor levamisole (Sigma Aldrich) was used in the concentration of 1 mM. Medium was changed every 3–4 days. The qPCR analyses were performed after 2 weeks. Oilred-O-staining and Alizarin-red staining were performed according to standard protocols after 3 and 4 weeks, respectively [26,27]. Quantification of the Oilred-O dye was performed adding 300 μ l isopropanol to the well (10 min, constant shaking on ice), followed by the measurement of triplicates using the GloMax[®] Multi-Detection System at 450 nm. The percentage of the area stained with Alizarin-red was calculated in ImageJ (Rasband, NIH, Bethesda, MD, USA) using an individual threshold.

2.3. RNA isolation, reverse transcription, and qPCRs

RNA was isolated using the Nucleo Spin[®] RNA Kit (Macherey-Nagel) according to manufacturer's instructions. Reverse transcription of 1 μ g RNA each was performed with the reverse transcriptase purchased from Promega according to standard protocols. For qPCR analysis, the GoTaq qPCR Mix (Promega) and the Opticon DNA engine (MJ Research) or the peqSTAR (PEQLAB) were used with the following standardized program (3 min 95°C, 40x [5 sec 95°C, 15 sec annealing-temperature (AT), 5 sec 72°C]; melting curve 45–95°C). Primer sequences and PCR conditions are listed in Appendix Table 1. The analysis of the obtained results was performed using the 2^{- Δ ct} method.

2.4. Determination of AP-activity (CSPD-Assay)

CSPD-assay was performed as previously described using CSPD ready-to-use reagent (0.25 mM) solution (Roche GmbH) [28].

2.5. FACS analysis

For analysis of typical MSC surface markers [29], cells isolated from the pulp and PDL of four donors (n = 4) were used in passage 2. Cells ($2-4 \times 10^5$ per tube) were stained with different antibodies (Appendix Table 2.) according to manufacturer's recommendations. Samples were analyzed at the LSR II Flow Cytometer (BD Bioscience) and data evaluated using the software FlowJo.

2.6. RNA-seq based transcriptome analysis

For analysis of the transcriptome, RNA samples, which have been extracted from the PDLSCs of five donors after two weeks of oD with and without the TNAP inhibitor levamisole (1 mM), were used. Library preparation was performed by the Core Unit Systems Medicine at University of Würzburg according to the Illumina TruSeq stranded mRNA Sample Preparation Guide with 500 ng of input RNA and 11 PCR cycles. All 10 libraries were pooled and sequenced on an Illumina NextSeq 500 with a read length of 75 nt. For details on the bioinformatic analysis see appendix.

Functional protein association networks were analyzed using STRING (<https://string-db.org/>). Detailed settings for the analysis are provided in the respective figure legends. Additionally, gene set enrichment analysis (GSEA) was performed online (<http://software.broadinstitute.org/gsea/index.jsp>) choosing the terms C5, C7, CP, CP:KEGG.

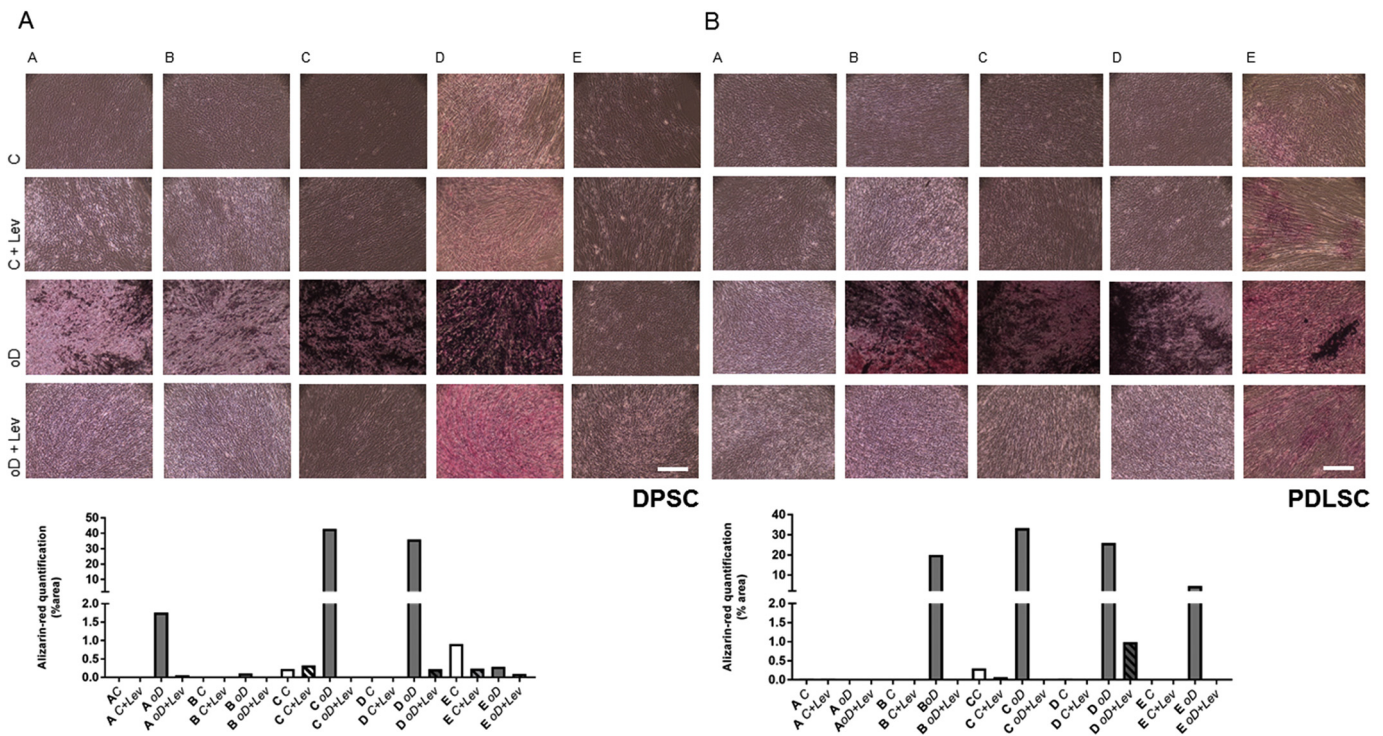


Fig. 1. Alizarin-red-staining of DPSCs (1A) and PDLSCs (1B) isolated from five donors (A–E) after four weeks of treatment with osteogenic differentiation medium. Graphs are depicting the quantification of Alizarin-red (in % area) that was performed with the program Image J. C = control, C + Lev = control treated with 1 mM levamisole, oD = osteogenic differentiation, oD + Lev = osteogenic differentiation treated with 1 mM levamisole. Scale bar: 250 μ m. Sample PDLSC A was only treated for 2.5 weeks since the cells had to be fixed and stained earlier due to beginning detachment.

2.7. Statistics

Statistics were calculated using the program GraphPad Prism 7. Depending on the respective Gaussian distribution, which was determined with the Kolmogorov-Smirnov-test, either a *t*-test or an ANOVA with Tukey Posthoc (if normal distribution could be proven) or a Mann-Whitney-U-test or Kruskal-Wallis with Dunn's Posthoc test (if the values were not normally distributed) were performed.

3. Results

3.1. DPSCs and PDLSCs express typical mesenchymal stem cell markers and show attributes of multipotency

Minimal criteria for MSCs were confirmed in all populations retrieved from teeth (Appendix Fig. 1). All populations showed both osteogenic and adipogenic differentiation capacity. The latter was however limited in comparison with bone marrow derived precursor cells. Bone marrow derived precursors were subjected to osteogenic differentiation protocols as a positive control (Appendix Fig. 2).

Levamisole abolished mineralization and supported concomitant expression of adipogenic genes when subjected to osteogenic differentiation protocols.

All samples showed proper Alizarin-red-staining after osteogenic differentiation, indicating robust mineralization capacity, except PDLSC A (Fig. 1B) (those cells were fixed after 2.5 weeks due to cell detachment), and DPSC E (Fig. 1A). The addition of the TNAP inhibitor levamisole (oD + Lev) abolished the mineralization process (Fig. 1).

Analysis of osteogenic (ALPL, ANKH, ENPP1, RUNX2, OC, OPN) and adipogenic (FABP, LPL, PPARG) marker genes during osteogenic and adipogenic differentiation showed higher expression by trend compared to the respective controls, albeit with high variability as expected (Fig. 2). The statistical evaluation of the respective effect of levamisole treatment is additionally shown in the appendix (Appendix Fig. 4).

Levamisole is a potent and dose-dependent inhibitor of TNAP (Appendix Fig. 3). Levamisole treatment, while abolishing mineralization *in vitro*, did not significantly change TNAP expression on mRNA levels in any of the analyzed populations (Fig. 2). ANKH and ENPP1 expression was lower in the presence of levamisole by oD day 14. Samples treated with aD medium showed low OPN expression. Runx2 expression was largely unaffected by levamisole treatment. Unexpectedly, the highest expression could be detected in DPSCs after aD treatment (Fig. 2). Levamisole treatment during oD enhanced co-expressed adipogenic marker genes especially in BMSCs, but suppressed the neurogenic stem cell marker NES in DPSCs.

Adipogenic marker genes like FABP4, LPL and PPARG2 were analyzed both during oD and aD. FABP4 and LPL (albeit on low level) expression levels were slightly higher after oD in BMSCs and PDLSCs and were further enhanced by levamisole treatment while PPARG was unchanged. In dental stem cells, typical marker gene expression was higher by trend during aD.

The neuronal stem cell marker NES showed the highest expression in DPSCs compared to the other cells. In controls and oD samples, the expression of NES was significantly higher in DPSCs than in BMSCs. In DPSCs, NES expression was lower in levamisole treated samples during osteogenic differentiation by trend. Nestin expression was untouched by levamisole treatment in control cells and even higher during oD conditions, but lower under TNAP inhibition by day 14 oD (Fig. 2 and Appendix Fig. 4).

In alkaline phosphatase activity tests of the samples harvested after 2 weeks of treatment (Appendix Fig. 5), some donor populations showed a higher AP-activity compared to control samples, which is indicating that under physiological conditions AP transcription and translation rates are regulated by a feedback loop as a consequence of inhibition of AP-activity by levamisole. This effect is due to the reversible binding characteristics of levamisole to the enzyme, where levamisole concentration is diluted or the inhibitor is even lost during sample preparation (for details see Appendix Fig. 3).

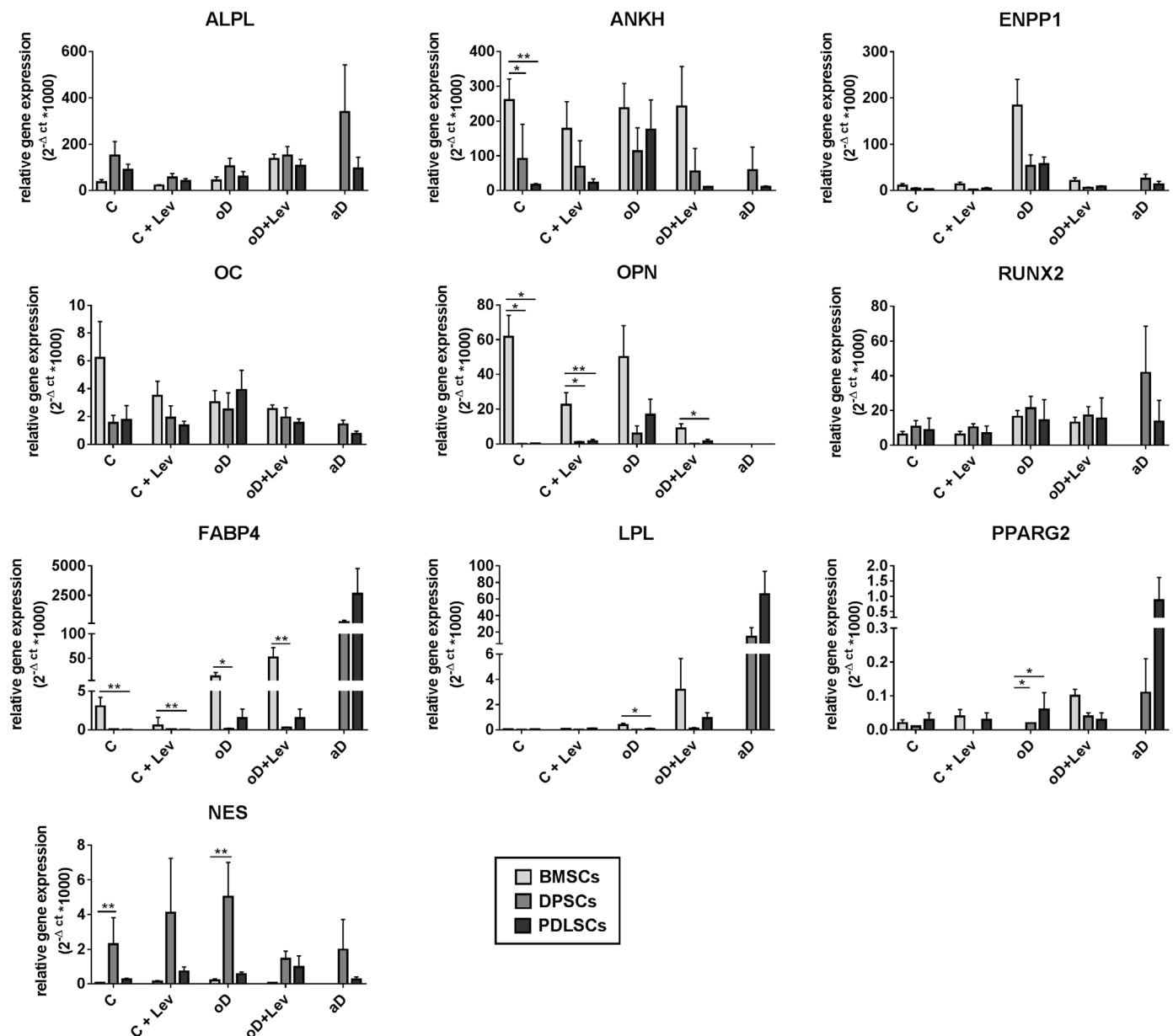


Fig. 2. Relative gene expression (displayed as $2^{-\Delta ct} * 1000$) shows the consequences of TNAP inhibition on gene expression after two weeks of osteogenic and adipogenic differentiation (aD not analyzed in BMSCs). Values for BMSCs, DPSCs and PDLSCs are depicted as mean \pm s.e.m. of the results obtained from five donors. All qPCRs were pipetted three times independently. Statistics were calculated for each treatment with ANOVA (Tukey Posthoc) if samples were distributed normally and with Kruskal-Wallis (Dunn's Posthoc) if not. *p < 0.05, **p < 0.01; C = control, C + Lev = control with 1 mM levamisole, oD = osteogenic differentiation, oD + Lev = osteogenic differentiation with 1 mM levamisole, aD = adipogenic differentiation; ALPL = tissue-nonspecific alkaline phosphatase, ANKH = ANKH inorganic pyrophosphate transport regulator; ENPP1 = ectonucleotide pyrophosphatase/phosphodiesterase 1, OC = osteocalcin, OPN = osteopontin, RUNX2 = runt related transcription factor 2, FABP4 = fatty acid binding protein 4, LPL = lipoprotein lipase, PPARG2 = peroxisome proliferator activated receptor gamma, NES = nestin.

3.2. RNA-seq analysis revealed anti-osteogenic and pro-inflammatory effects of levamisole treatment in the PDLSC population

RNA-seq analysis was conducted on five donor specimens of PDLSCs used for the osteogenic differentiation experiments (day 14). The RNA-seq data is publicly available in NCBI's Gene Expression Omnibus [30] (for details see section Data availability). Additionally, a list of the up- and downregulated genes is provided in the appendix (Appendix Table 3). The following figure shows a heatmap of the genes significantly regulated with a log fold change > 2 (Fig. 3A) and a table with nine selected candidate genes of interest (Fig. 3B). Lead genes of interest were selected from RNA-seq results due to their role in bone metabolism and purinergic signaling and are depicted in Fig. 3B.

Additionally, principal components analysis (PCA) plot, representing the RNA-seq results (Fig. 3C), and the validation of selected genes of interests via qPCR are depicted in Fig. 3D.

The heatmap gene regulation pattern is consistent (Fig. 3A), apart from sample PDLSC A oD (first column). The PCA plot confirmed that the two groups of analyzed samples (PDLSC oD and PDLSC oD + Lev) clustered properly, apart from PDLSC oD sample A and PDLSC oD + Lev sample D, which showed a different distribution pattern compared to the other samples of the respective group and could be considered as outliers (Fig. 3C). An additional analysis of the differences between PDLSC oD sample A and the rest of the samples can be seen in the Appendix. The qPCR results depicted in Fig. 3D confirmed the trends that have already been indicated by RNA-seq analysis.

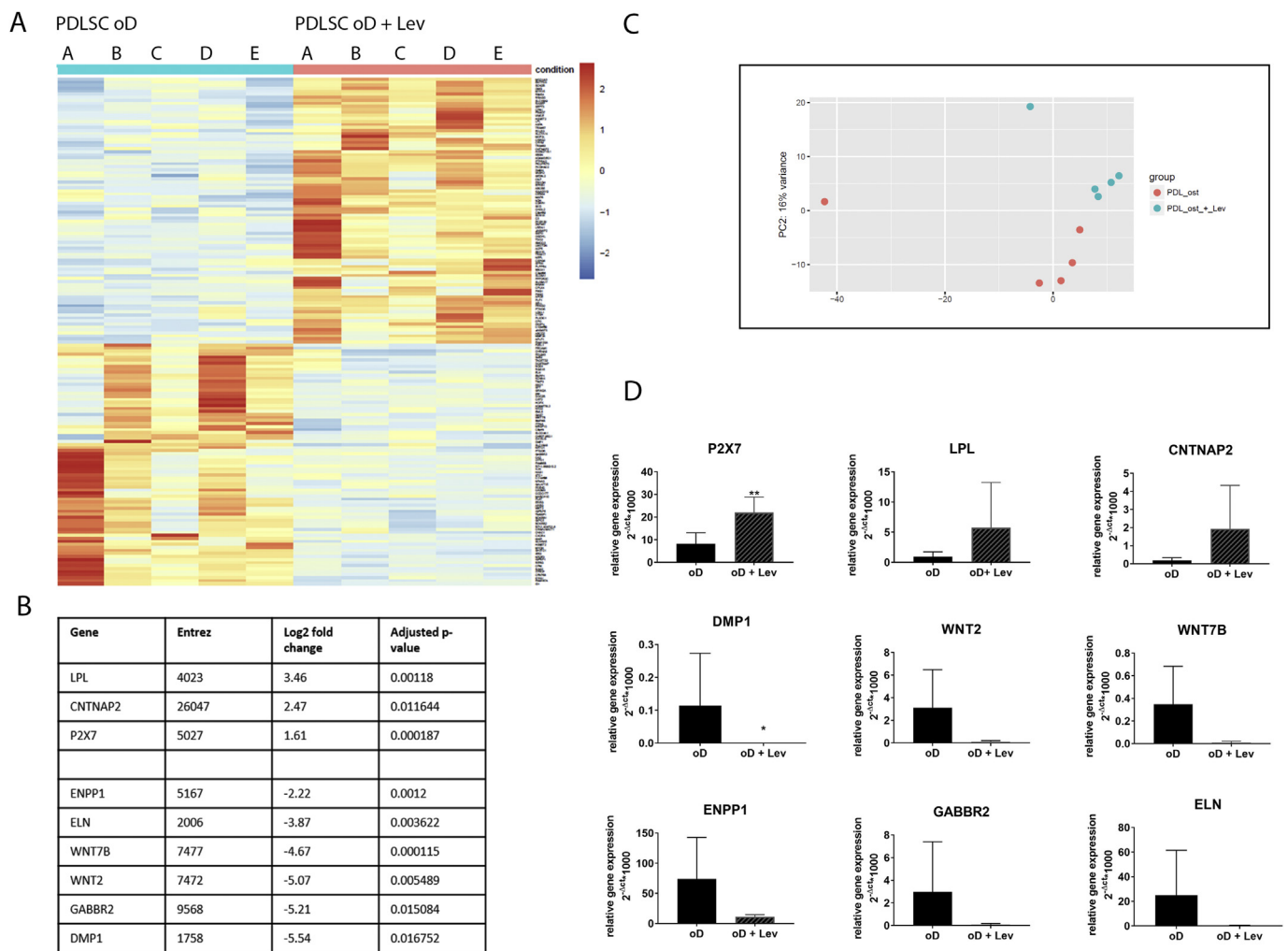


Fig. 3. A: Heatmap depicting clustering of differentially expressed genes from RNA-seq analysis of PDLSCs of five different donors after two weeks of osteogenic differentiation with and without treatment of 1 mM levamisole. Red color symbolizes up- and blue downregulation of the respective gene; each row depicts the results of one sample. The five samples on the left were treated with osteogenic differentiation medium only; the five samples on the right were additionally treated with 1 mM levamisole. The heatmap includes RNAseq results that fit the following criteria: p -value < 0.05 , \log_2 fold-change > 2 or < -2 , respectively. **B:** Nine selected genes of interest that show differential expression in RNA-seq analysis. **C:** Principal component analysis (PCA) plot showing the clustering pattern of two groups (PDLSC oD and PDLSC oD + Lev). Each dot represents a biological sample. The color code corresponds to the respective group type. Percentage on PCA axis represents the percentage variance. **D:** qPCR analysis for validation of the influence of levamisole treatment during oD in PDLSCs. Depicted are the means \pm s.d. of relative gene expression values of five different donors. All qPCRs were pipetted three times independently. Statistics were calculated with t -test or two-tailed Mann-Whitney-U-test (depending on the respective Gaussian distribution). * $p < 0.05$, ** $p < 0.01$; P2X7 = purinergic receptor P2X 7, LPL = lipoprotein lipase, CNTNAP2 = contactin associated protein like 2, DMP1 = dentin matrix protein 1, WNT2 = Wnt family member 2, WNT7B = Wnt family member 7B, ectonucleotide pyrophosphatase/phosphodiesterase 1, GABBR2 = gamma-aminobutyric acid type B receptor subunit 2, ELN = elastin.

Statistically significant expression changes caused by levamisole treatment during oD could be seen in an increase of purinergic receptor P2X7 as well as a decrease of DMP1 expression in PDLSCs.

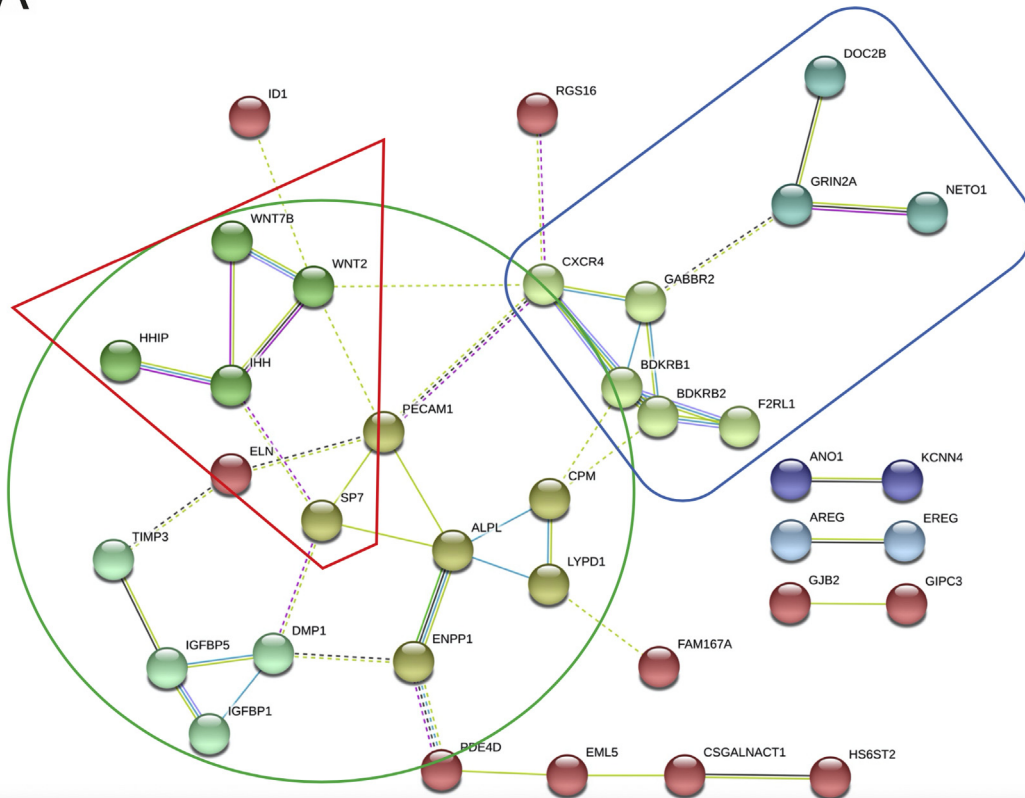
The protein network analysis of all regulated as well as only the genes that were downregulated in RNA-seq comparing PDLSCs after 2 weeks of osteogenic differentiation with and without inhibition of TNAP-activity (Fig. 4 and Appendix Fig. 6), illustrated the interactions between core osteogenic genes, mineralization and phosphate household regulators (DMP1, SP7, PDE4D, ENPP1), genes involved in matrix protein turnover and degradation (ELN, TIMP3), neuronal and inflammatory genes (GABBR2), and genes involved in bone growth and development (IHH, HHIP, WNT2, WNT7B, SP7, DMP1, IGFBP5, IGFBP1, TIMP3). A more detailed description of the complete network is given in the Appendix, as well as the technical settings in the STRING program that allow for detailed viewing of the interaction and the multiple additional pathway analyses given by this program.

Additionally performed GSEA analysis of the 81 significantly up-

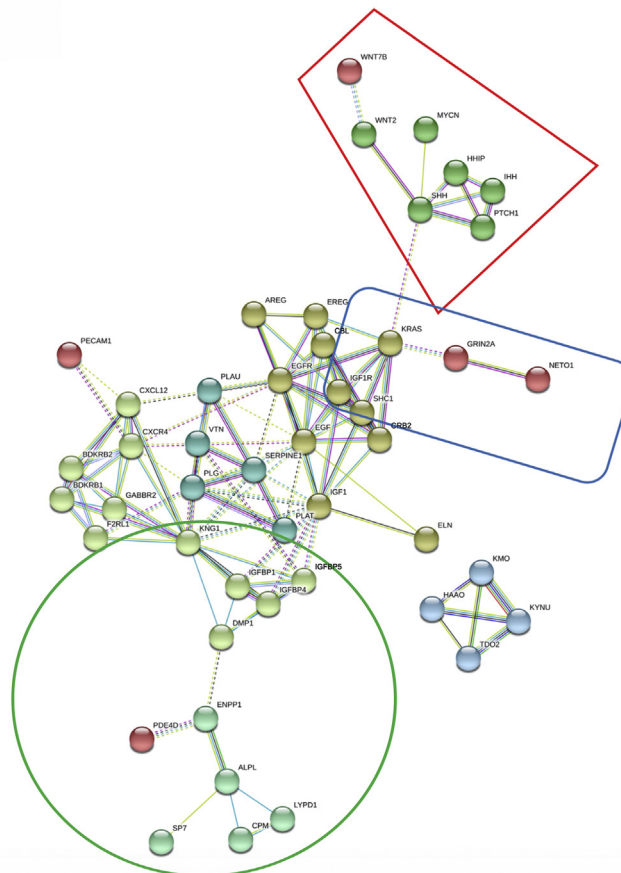
and 74 downregulated genes (p -value < 0.05 , \log_2 fold-change > 2 or < -2) revealed a significant overlap of 33 regulated genes with the terms extracellular space and intrinsic component of plasma membrane. Additionally, 31 genes were related to tissue development, 28 to receptor binding, and 25 to membrane region. Analysis of upregulated gene list showed a significant overlap of 14 genes with the term neurogenesis and nine with neuron projection development. The neuronal cell adhesion protein CNTNAP2 represented an example for the latter.

Although there was no clear signal in the GSEA analysis for adipogenesis, lipoprotein lipase again appeared in the RNA-seq pattern as an upregulated gene in the presence of levamisole. As elastin is an important elastic component of the periosteum, we also analyzed the expression of elastin as a candidate. Here only 2 out of 5 donors clearly showed a positive signal for ELN in osteogenic differentiation sample, which was downregulated under levamisole treatment. In this context, the interaction between elastin and the TIMP metalloproteinase inhibitor 3 (TIMP3) (Fig. 4) is of relevance since the background

A



B



(caption on next page)

Fig. 4. Network analysis for protein interaction of downregulated genes in RNA-seq comparing PDLSCs after 2 weeks of osteogenic differentiation with and without levamisole treatment performed with STRING. Downregulated genes and clusters (A) and adding 2x10 protein interaction partners in a first and second shell (B). Performing a STRING protein interaction analysis, we find clusters of downregulated genes related to core osteogenic signaling (A, query genes only) (red lines) as well as supportive signaling for osteoblast/osteocyte maturation and mineralization (green lines) comparing PDLSCs after 2 weeks of osteogenic differentiation with and without levamisole treatment. Blue circles mark a cluster of neurotrophic and inflammatory signaling genes (Settings: evidence, interaction score = medium confidence 0.400; no interactors; disable structure previews; hide disconnected nodes; number of clusters = 10). When allowing the system to add classical interaction partners to scheme (B) (Settings: evidence, interaction score = high confidence 0.700; no more than 10 interactors on both shells; disable structure previews; hide disconnected nodes; number of clusters = 10) we obtain even more markedly clustering osteosupportive genes, which are linked by added peptide ligands such as EGF and IGF1, whereas the core osteogenic pathway genes of the wnt and hedgehog signaling cascades appear to be somewhat separated from the late osteocyte/mineralization cluster (green line). In addition, the early and late osteogenic cluster get separated by an inflammation/matrix metabolism cluster that is fostered by adding a limited number of classical interaction partners. Interestingly, parts of the neurogenic cluster (e.g. GABBR2 and F2RL1) are recruited to the inflammation cluster when adding more interactive partners. If interested readers use the publicly available STRING program with the settings provided, this allows detailed views, including interactive gene information, when clicking on the respective gene nodes.

information (as also discussed below) for interaction evidence comprised important protein interaction of TIMP3 and elastin as well as TIMP3 and the osteogenic differentiation program.

3.3. New genes responsive to TNAP inhibition were comparably regulated in the populations derived from pulp and ligament

In order to compare the effects of levamisole treatment between populations with respect to the new candidate genes, we additionally analyzed cDNA samples from the pulp stem cell populations under osteogenic differentiation conditions with and without levamisole treatment using qPCR (Fig. 5). The plotted data for PDLSC were analogous to the ones depicted in Fig. 3D.

Genes of relevance for the osteogenic and purinergic signaling pathways as well as PP₁ regulation (WNT2, WNT7B, ENPP1, DMP1, and P2X7) showed similar trends if directly compared, albeit on different expression levels. Also, markers for neurogenic and adipogenic differentiation (GABBR2, CNTNAP2, and LPL) showed similar trends in pulp derived stem cells and thus confirmed the results obtained from RNA-seq in the ligament derived population. Additionally performed experiments with the alternative TNAP inhibitor MLS-0038949 showed similar results (data not shown). This decreases the likelihood of the levamisole results being substantially influenced by levamisole side effects.

4. Discussion

We showed here that inhibition of TNAP activity in dental precursor cells results in gene regulation patterns that are compatible with impaired osteogenesis/mineralization, altered neuronal signaling and enhanced inflammation/ECM turnover and degradation. These cells showed attributes of multipotency and met the minimal requirement surface marker characteristics for skeletal precursors, so called MSCs. PDL-derived populations showed properties of pericytes (expression of CD146) [31] and displayed a higher osteogenic than adipogenic differentiation capacity [32]. Although we see the usual donor variability of primary cultures, we can demonstrate that *in vitro* mineralization was consistently abolished during TNAP inhibition. Expression of RUNX2 as a core osteogenic transcription factor was largely unchanged, indicating that the osteogenic commitment was maintained apart from osteoblast development and mineralization. Even though the different donors show a certain variability, the PDL cells and the pulp cells were able to mineralize.

In vitro and *in vivo* mineralization reflects a very complex interaction of maybe 10–15 core partner molecules, where TNAP certainly is most relevant and provides Pi for crystallization [7,33]. As we can demonstrate in Fig. 2, there is also evidence for a local regulatory loop involving e.g. TNAP, ENPP1, SPP1 (alias OPN, osteopontin) and ANKH. The multifaceted process is very variable in individuals representing also the basis of interindividual heterogeneity of mineralization capacity in primary cultures of skeletal precursors. Osteopontin (SPP1) is one example of a very strong modulator of mineralization. SPP1-

derived phosphorylated polypeptides are substrates of TNAP and modulate mineralization dependent on their phosphorylation state. This was impressively demonstrated by the partial rescue effect in *Alpl* deficient mice that came along with the additional osteopontin knockout [34]. The substrate and product changes related to TNAP activity have been published by Ren et al. who have already analyzed the levels of different phosphate substrates depending on TNAP activity in osteoblasts and matrix vesicles via infrared spectroscopy [35]. The resulting changes in signaling via e.g. purinergic pathways or phosphate sensing upon TNAP inhibition are part of our research question as they precipitate in an altered transcriptome signature, which we captured and described. The recruited and cooperating enzymes and modulators dynamically change the microenvironment and local concentrations of phosphate compounds that are certainly diluted by cell culture fluids or tissue-derived fluids *in vivo* along the distance to the enzymes. We strongly believe that this scenario is exactly the one we anticipated and the resulting transcriptional changes mirror the *in vivo* conditions.

PDL cells were chosen as the most representative model for in depth analysis of the molecular pathology in HPP since they contribute to cementum and ligament formation [31]. Hence, premature loss of deciduous teeth with impaired tooth root resorption in HPP [11] may be explained with alterations in the periodontium and cementum, including effects of decreased TNAP activity on mineralization processes as well as on the expression of ECM components. RNA-seq analysis and confirmatory qPCR in PDLSCs revealed significant downregulation of core components of cascades involved in osteogenic and neuronal differentiation. Effective alteration of osteogenic and neuronal signaling may reduce the amount of cementum formed, which determines the size of the contact area between tooth roots and surrounding bone [12]. We found downregulation of e.g. the osteoblast-specific transcription factor *Osx/SP7* as well as of components that are important for wnt, hippo and hedgehog signaling besides others that are relevant for osteoblast development and maturation like DMP1, ENPP1 as well as EGF and IGF1. DMP1 loss of function mutations lead to autosomal recessive hypophosphatemic rickets including severe tooth problems [36]. The significant downregulation of DMP1 expression by TNAP inhibition may contribute to the inhibition of dentin and cementum mineralization [37].

Additionally, we intended to elucidate the influence of levamisole treatment on molecular processes beyond mineralization. Several genes that are directly or indirectly involved in regulation of inflammatory processes were found to be differentially regulated depending on the absence or presence of levamisole. DMP1, which was found to be downregulated, has a protective effect against inflammation and can therefore contribute to the enhancement of inflammation under TNAP inhibition. Additionally, eATP is increased due to substrate accumulation during TNAP inhibition [38]. Moreover, the downregulation of ENPP1 may further promote chronic inflammatory processes due to its capability to dephosphorylate ATP that was recently confirmed in structural analyses [39]. Taken together, the inhibition of TNAP and downregulation of ENPP1 expression leads to an enhanced

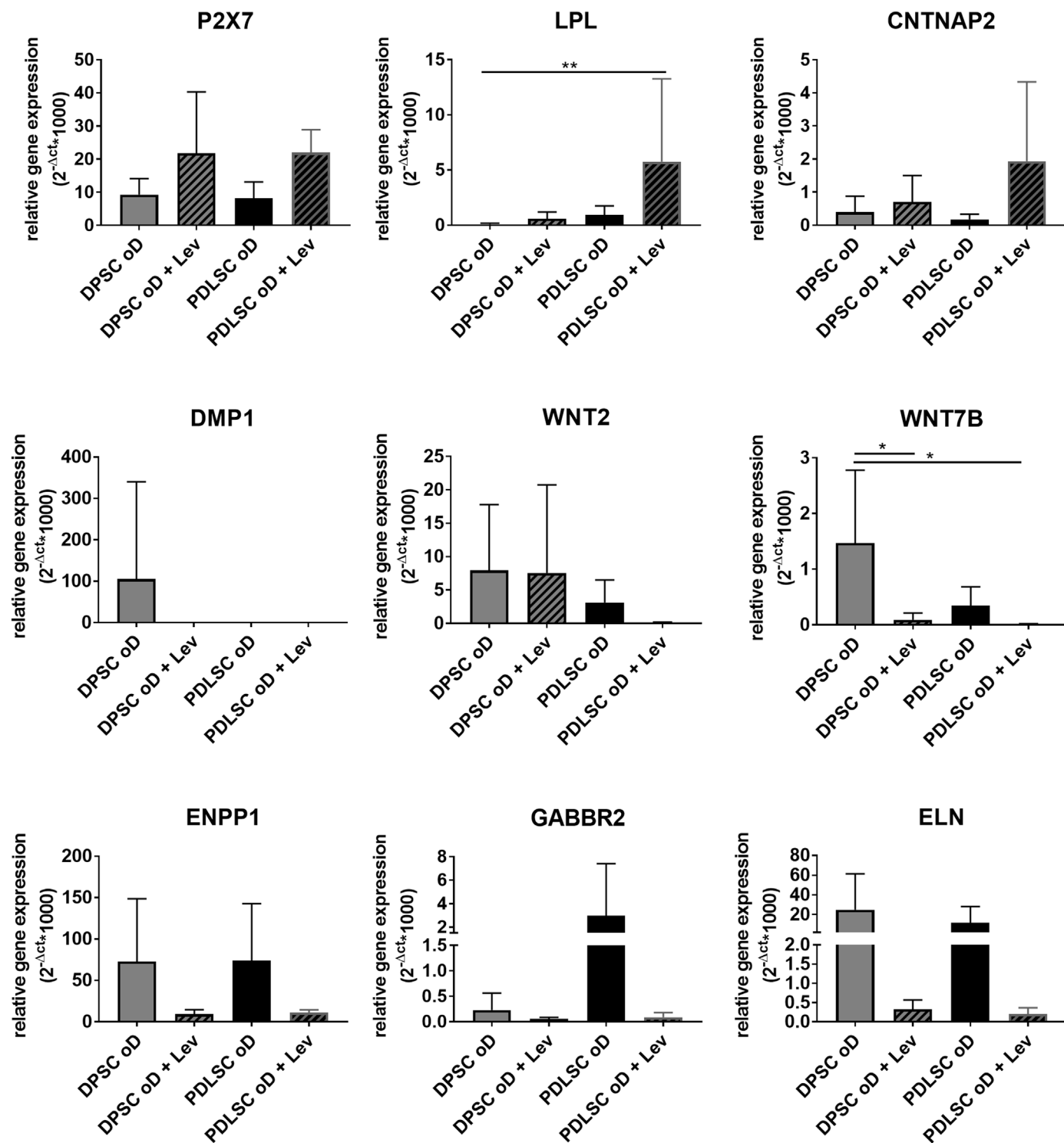


Fig. 5. Comparison of levamisole effects after two weeks of oD in DPSCs and PDLSCs. Depicted are the means \pm s.d. of relative gene expression of five different donors. The plotted data for PDLSC are also depicted in Fig. 6D. Statistics were calculated with ANOVA (Tukey Posthoc) test. *p < 0.05, **p < 0.01; P2X7 = purinergic receptor P2X7, LPL = lipoprotein lipase, CNTNAP2 = contactin associated protein like 2, DMP1 = dentin matrix protein 1, WNT2 = Wnt family member 2, WNT7B = Wnt family member 7B, ectonucleotide pyrophosphatase/phosphodiesterase 1, GABBR2 = gamma-aminobutyric acid type B receptor subunit 2, ELN = elastin.

accumulation of eATP, which fuels inflammation via binding to P₂X₇ receptors [40]. This may be even more effective in sustaining pathology since we also find upregulation of the purinergic P2X7 gene, one of several ATP receptors. The resulting inflammatory effect stimulating the activity of the inflammasome would at least neutralize the basically positive effects of receptor activation on bone maintenance as described

in the P₂X₇ knockout models [41,42].

Dental tissue related precursor populations are derived from neuroectodermal tissues, hence neuron-related signaling may be more important than in bone marrow derived populations. Recent research describes the relevance of neuropeptide signaling for bone protection but also for pro-inflammatory signaling of neuropeptide and small

molecule ligands of respective receptors [43]. Neurotrophic factors like BDNF are discussed for regeneration of cementum and ligament [44] and GABBR2 receptor KO enhances periodontal bone loss [45]. GABBR2, F2RL1 trypsin receptor BDKRB1 and 2 form a downregulated cluster in the protein interaction analysis. As we showed, similar effects can be seen in neuronal cells (SH-SY5Y) with low versus forced over-expression of TNAP ([28] and unpublished data). The complexity of neuron-specific signal transduction in terms of protection versus inflammation remains to be elucidated.

We also find alteration of components of the ECM and its turnover, which should be extremely relevant in the ligament function of the PDL like the downregulation of elastin (ELN). ELN is an important elastic component of the fibrous layer of the periosteum and was, among others, described to play a role in periodontal regeneration [46,47]. The combination of collagen and elastin determines the mechanical properties of the periosteum and Sharpey's fibers, which are above all composed of collagen, are indispensable for the anchorage of the periosteum to the bone [46]. Elastin as a scaffold was reported to increase TNAP activity and may have an influence on intrafibrillar calcification at insertions [48]. Moreover, we also found that TIMP3, an important modulator of ECM turnover, was also downregulated by TNAP inhibition. TIMP3^{-/-} mice develop aortic aneurysms due to increased elastin degradation on the protein level, indicating that deficient TIMP3 activity leads to severely altered elasticity of the aortic wall [49], which could happen in analogy in altered PDL function in HPP and result in slackening and consecutive exfoliation of teeth.

Using the STRING based analysis of protein interactions, the results always comprise significantly more interactions than could be expected. Even though this extremely complex program, which is powered by big data from the literature in the background, might create more and more speculative results if overdone, the level of our analysis is rather plausible and inspiring, opening up new routes of research in this field.

The A116T knock-in mouse has been established as a specific mouse model for Odonto-HPP [50]. Despite their decreased AP-activity, these mice did not show striking skeletal abnormalities, apart from changes in the alveolar and cranial bones [50]. The cellular cementum was abnormal and the acellular cementum of molars and incisors was decreased by a non-significant trend [50]. Even though the mice did not show severe dentin and enamel defects or premature loss of teeth [50], the results gained from this mouse model support our own results, indicating a higher number of mechanisms that are influenced by TNAP enzyme. Taken together, the craniofacial system, including the teeth, under certain predisposing conditions like the presence of an *ALPL* mutation and inflammation triggered loss of alveolar bone and cementum, seems to be more susceptible to decreased TNAP activity than the skeleton.

A disputable weakness of our study is the inter-individual variability of gene expression, where the relatively low number of individual donors for various parameters does not achieve statistical significance. In order to get an impression on the differences between the outlier donor A PDL and the other four samples, we performed an additional GSEA analysis that revealed, among others, differences concerning genes of the cluster "ossification", which is in line with our results (see Appendix and the supplemental excel files Appendix_Donor_A_GSEA_high and Appendix_Donor_A_GSEA_low). Nevertheless, donor variability is a standard concern in research with primary material. Furthermore, chondrogenic differentiation assays, in order to confirm the three-lineage differentiation capacity, were skipped due to the scarcity of cell material and due to the same reason FACS analyses were performed with four samples differing from the ones that were used for RNA-seq, qPCRs and differentiation assays.

In summary, a core set of genes related to bone formation was suppressed in these early regenerative dental cell populations when TNAP activity was inhibited, suggestive not only for impaired mineralization capacity, but also for impaired osteoblast maturation. Additionally, a cascade of events triggers pro-inflammatory activity

that certainly contributes to bone loss in the complex filigree system of tooth anchorage that consists of bone and ligament components. The latter may be severely altered by dysregulation of ECM turnover and e.g. degradation of ELN, impairing its elastic features. This may further propagate ligament rupture and exfoliation of teeth. Although enzyme replacement therapy or bone anabolic treatment are available for a selected patient population, our data stimulate future research about targeting the dental problems in HPP of any severity, locally or systemically.

CRediT authorship contribution statement

Hannah Melms: Investigation, Methodology, Validation, Formal analysis, Investigation, Visualization, Writing - original draft. **Marietta Herrmann:** Investigation, Formal analysis, Visualization, Writing - review & editing. **Konrad Förstner:** Writing - review & editing, Formal analysis. **Richa Bharti:** Formal analysis, Investigation, Writing - original draft, Visualization. **Doris Schneider:** Investigation. **Birgit Mentrup:** Methodology, Writing - review & editing. **Maximilian Rudert:** Writing - review & editing. **Ulrich Schlagenhaut:** Writing - review & editing. **Franz Jakob:** Conceptualization, Writing - original draft, Supervision, Project administration, Funding acquisition. **Stephanie Graser:** Conceptualization, Writing - original draft, Supervision, Project administration, Funding acquisition, Visualization.

Declaration of competing interest

Franz Jakob received honoraria for lectures and advice from Alexion. Apart from this, no competing interests need to be declared.

Acknowledgement

We thank the surgeons from Orthopedic Department König-Ludwig-Haus Würzburg and from the Dentistry Department, University Clinics Würzburg for providing the patient material after surgery and AG Walles for providing the ethics permission for the isolation of dental stem cells. We thank Hypophosphatasie Deutschland e.V. for providing the financial support for this project.

Appendix A. Supplementary data

Supplementary data to this article can be found online at <https://doi.org/10.1016/j.yexcr.2020.112026>.

Funding

This research received no specific grant from any funding agency in the public, commercial or non-for-profit sectors. It was financially supported by Europäischer Fonds für regionale Entwicklung (EFRE) (grant EU-1650-0006) and by donations from Hypophosphatasie Deutschland e.V. Stephanie Graser is funded by the Deutsche Forschungsgemeinschaft (DFG, German Research Foundation) – project number 397519724. Marietta Herrmann is funded by Interdisciplinary Center for Clinical Research (IZKF) at the University of Würzburg (Project D-361).

Data availability

The RNA-seq data discussed in this publication has been deposited in NCBI's Gene Expression Omnibus [30] and are accessible through GEO Series accession number GSE131338 (<https://www.ncbi.nlm.nih.gov/geo/query/acc.cgi?acc=GSE131338>).

Summary

Alkaline phosphatase inhibition in dental pulp and ligament stem cells impairs osteogenic differentiation while favoring adipogenesis, pro-inflammatory purinergic signaling and ECM degradation – an *in vitro* modelling system for dental defects in hypophosphatasia was established.

References

- [1] E. Mornet, et al., A molecular-based estimation of the prevalence of hypophosphatasia in the European population, *Ann. Hum. Genet.* 75 (3) (2011) 439–445.
- [2] M.P. Whyte, Hypophosphatasia: an overview for 2017, *Bone* 102 (2017) 15–25.
- [3] A. Reibel, et al., Orofacial phenotype and genotype findings in all subtypes of hypophosphatasia, *Orphanet J. Rare Dis.* 4 (2009) 6.
- [4] H. Liu, et al., Genetic etiology and dental pulp cell deficiency of hypophosphatasia, *J. Dent. Res.* 89 (12) (2010) 1373–1377.
- [5] E. Mornet, *Hypophosphatasia*. *Metabolism* 82 (2018) 142–155.
- [6] H. Zimmermann, M. Zebisch, N. Strater, Cellular function and molecular structure of ecto-nucleotidases, *Purinergic Signal.* 8 (3) (2012) 437–502.
- [7] D. Harmey, et al., Concerted regulation of inorganic pyrophosphate and osteopontin by Akp2, Enpp1, and Ank - an integrated model of the pathogenesis of mineralization disorders, *Am. J. Pathol.* 164 (4) (2004) 1199–1209.
- [8] K. Hoshi, et al., Immunolocalization of tissue non-specific alkaline phosphatase in mice, *Histochem. Cell Biol.* 107 (3) (1997) 183–191.
- [9] M. Goseki-Sone, et al., Expression of mRNA encoding tissue-nonspecific alkaline phosphatase in human dental tissues, *Calcif. Tissue Int.* 64 (2) (1999) 160–162.
- [10] L.E. Zweifler, et al., Counter-regulatory phosphatases TNAP and NPP1 temporally regulate tooth root cementogenesis, *Int. J. Oral Sci.* 7 (1) (2015) 27–41.
- [11] L.L. Chapple, Hypophosphatasia: dental aspects and mode of inheritance, *J. Clin. Periodontol.* 20 (9) (1993) 615–622.
- [12] A. Olsson, et al., Hypophosphatasia affecting the permanent dentition, *J. Oral Pathol. Med.* 25 (6) (1996) 343–347.
- [13] H.U. Luder, Malformations of the tooth root in humans, *Front. Physiol.* 6 (2015) 307.
- [14] P. Bianco, P.G. Robey, P.J. Simmons, Mesenchymal stem cells: revisiting history, concepts, and assays, *Cell Stem Cell* 2 (4) (2008) 313–319.
- [15] P. Robey, Mesenchymal Stem Cells: Fact or Fiction, and Implications in Their Therapeutic Use *F1000Res* (2017) 6.
- [16] M. Herrmann, F. Jakob, Bone marrow niches for skeletal progenitor cells and their inhabitants in health and disease, *Curr. Stem Cell Res. Ther.* 14 (4) (2019) 305–319.
- [17] S. Gronthos, et al., Postnatal human dental pulp stem cells (DPSCs) *in vitro* and *in vivo*, *Proc. Natl. Acad. Sci. U. S. A.* 97 (25) (2000) 13625–13630.
- [18] Y. Chai, et al., Fate of the mammalian cranial neural crest during tooth and mandibular morphogenesis, *Development* 127 (8) (2000) 1671–1679.
- [19] A. Baudry, et al., Serotonin in Stem Cell Based-Dental Repair and Bone Formation: A Review, *Biochimie*, 2018.
- [20] T.L. Rodrigues, et al., Correction of hypophosphatasia-associated mineralization deficiencies *in vitro* by phosphate/pyrophosphate modulation in periodontal ligament cells, *J. Periodontol.* 83 (5) (2012) 653–663.
- [21] T.L. Rodrigues, et al., Hypophosphatasia-associated deficiencies in mineralization and gene expression in cultured dental pulp cells obtained from human teeth, *J. Endod.* 38 (7) (2012) 907–912.
- [22] U. Schlagenhauf, Professional Dissertation, Eberhard-Karls-Universität Tübingen, 1992.
- [23] J. Karbanova, et al., Characterization of dental pulp stem cells from impacted third molars cultured in low serum-containing medium, *Cells Tissues Organs* 193 (6) (2011) 344–365.
- [24] R. Ebert, et al., Acute phase serum amyloid A induces proinflammatory cytokines and mineralization via toll-like receptor 4 in mesenchymal stem cells, *Stem Cell Res.* 15 (1) (2015) 231–239.
- [25] B. Klotz, et al., 1,25-dihydroxyvitamin D3 treatment delays cellular aging in human mesenchymal stem cells while maintaining their multipotent capacity, *PLoS One* 7 (1) (2012) e29959.
- [26] M.F. Pittenger, et al., Multilineage potential of adult human mesenchymal stem cells, *Science* 284 (5411) (1999) 143–147.
- [27] U. Noth, et al., Multilineage mesenchymal differentiation potential of human trabecular bone-derived cells, *J. Orthop. Res.* 20 (5) (2002) 1060–1069.
- [28] S. Graser, et al., Overexpression of tissue-nonspecific alkaline phosphatase increases the expression of neurogenic differentiation markers in the human SH-SY5Y neuroblastoma cell line, *Bone* 79 (2015) 150–161.
- [29] M. Dominici, et al., Minimal criteria for defining multipotent mesenchymal stromal cells. The International Society for Cellular Therapy position statement, *Cytotherapy* 8 (4) (2006) 315–317.
- [30] R. Edgar, M. Domrachev, A.E. Lash, Gene Expression Omnibus: NCBI gene expression and hybridization array data repository, *Nucleic Acids Res.* 30 (2002) 207–210.
- [31] B.M. Seo, et al., Investigation of multipotent postnatal stem cells from human periodontal ligament, *Lancet* 364 (9429) (2004) 149–155.
- [32] K. Otobe, et al., Comparison of gingiva, dental pulp, and periodontal ligament cells from the standpoint of mesenchymal stem cell properties, *Cell Med.* 4 (1) (2012) 13–21.
- [33] M.C. Yadav, et al., Ablation of osteopontin improves the skeletal phenotype of phospho1(-/-) mice, *J. Bone Miner. Res.* 29 (11) (2014) 2369–2381.
- [34] D. Harmey, et al., Elevated skeletal osteopontin levels contribute to the hypophosphatasia phenotype in Akp2(-/-) mice, *J. Bone Miner. Res.* 21 (9) (2006) 1377–1386.
- [35] Z. Ren, et al., Direct determination of phosphatase activity from physiological substrates in cells, *PLoS One* 10 (3) (2015) e0120087.
- [36] A. Rangiani, et al., Dentin matrix protein 1 and phosphate homeostasis are critical for postnatal pulp, dentin and enamel formation, *Int. J. Oral Sci.* 4 (4) (2012) 189–195.
- [37] M.D. McKee, et al., Extracellular matrix mineralization in periodontal tissues: noncollagenous matrix proteins, enzymes, and relationship to hypophosphatasia and X-linked hypophosphatemia, *Periodontol* 63 (1) (2000) 102–122 2013.
- [38] R. Huizinga, et al., Endotoxin- and ATP-neutralizing activity of alkaline phosphatase as a strategy to limit neuroinflammation, *J. Neuroinflammation* 9 (2012) 266.
- [39] K. Kato, et al., Structural insights into cGAMP degradation by Ecto-nucleotide pyrophosphatase phosphodiesterase 1, *Nat. Commun.* 9 (1) (2018) 4424.
- [40] G. Burnstock, G.E. Knight, The potential of P2X7 receptors as a therapeutic target, including inflammation and tumour progression, *Purinergic Signal.* 14 (1) (2018) 1–18.
- [41] H.Z. Ke, et al., Deletion of the P2X7 nucleotide receptor reveals its regulatory roles in bone formation and resorption, *Mol. Endocrinol.* 17 (7) (2003) 1356–1367.
- [42] M. Carluccio, et al., Involvement of P2X7 receptors in the osteogenic differentiation of mesenchymal stromal/stem cells derived from human subcutaneous adipose tissue, *Stem Cell Rev*, 2019.
- [43] S. Grassel, D. Muschter, Do neuroendocrine peptides and their receptors qualify as novel therapeutic targets in osteoarthritis? *Int. J. Mol. Sci.* 19 (2) (2018).
- [44] R. Jimbo, et al., Regeneration of the cementum and periodontal ligament using local BDNF delivery in class II furcation defects, *J. Biomed. Mater. Res. B Appl. Biomater.* 106 (4) (2018) 1611–1617.
- [45] T.O. Goncalves-Zillo, et al., Increased bone loss and amount of osteoclasts in kinin B1 receptor knockout mice, *J. Clin. Periodontol.* 40 (7) (2013) 653–660.
- [46] N.Y. Yu, et al., Live tissue imaging to elucidate mechanical modulation of stem cell niche quiescence, *Stem Cells Transl Med* 6 (1) (2017) 285–292.
- [47] S. Ivanovski, et al., Gene expression profiling of cells involved in periodontal regeneration, *Tissue Eng.* 13 (2) (2007) 393–404.
- [48] N. Mizutani, et al., The behavior of ligament cells cultured on elastin and collagen scaffolds, *J. Artif. Organs* 17 (1) (2014) 50–59.
- [49] R. Basu, et al., Loss of Timp3 gene leads to abdominal aortic aneurysm formation in response to angiotensin II, *J. Biol. Chem.* 287 (53) (2012) 44083–44096.
- [50] B.L. Foster, et al., Periodontal defects in the A116T knock-in murine model of odontohypophosphatasia, *J. Dent. Res.* 94 (5) (2015) 706–714.